https://doi.org/10.5194/tc-2023-15
Preprint. Discussion started: 15 February 2023

The Cryosphere Discussions

Coupling the regional climate MAR model with the ice sheet model PISM mitigates the melt-elevation positive feedback

Alison Delhasse [1], Johanna Beckmann [2], Christoph Kittel [3,1], and Xavier Fettweis [1]

[1]Laboratory of Climatology, Department of Geography, SPHERES, University of Liège, Liège, Belgium
[2]Climate Impact Research (PIK), Member of the Leibniz Association, Potsdam, Germany
[3]Institut des Géosciences de l'Environnement (IGE), Université Grenoble Alpes/CNRS/IRD/G-INP, Grenoble, France

Correspondence to: Alison Delhasse (alison.delhasse@uliege.be)

Abstract. The Greenland Ice Sheet is a key contributor to sea level rise. By melting, the ice sheet thins, inducing higher surface melt due to lower surface elevations, accelerating the melt coming from global warming. This process is called the melt-elevation feedback that can be considered by using two types of models: atmospheric models, which can represent the surface mass balance, usually using a fixed surface elevation, and the ice sheet models, which represent the surface elevation evolution but do not represent the surface mass balance as well as atmospheric models. A new coupling between the regional climate model MAR (Modèle Atmosphérique Régional) and the ice sheet model PISM (Parallel Ice Sheet Model) is presented here following the CESM2 (SSP5-8.5) scenario until 2100 at the MAR lateral boundaries. The coupling is extended to 2200 with a stabilised climate (+ 7 °C compared to 1961 – 1990) by randomly sampling the last 10 years of CESM2 to force MAR and reaches a sea level rise contribution of 64 cm. The fully coupled simulation is compared to a 1-way experiment where surface topography remains fixed in MAR. However, the surface mass balance is corrected to the melt-elevation feedback when extrapolated on the PISM grid by using surface mass balance vertical gradients as a function of local elevation variations (offline correction). This method is often used to represent the melt-elevation feedback and avoid a coupling expensive in computation time. In the fully-coupled MAR simulation, the ice sheet morphology evolution (changing slope and reducing the orographic barrier) induces changes in local atmospheric circulation. More specifically, wind regimes are modified which influences the melt rate at the ice sheet margins. We highlighted a mitigation of the melt lapse rate on the margins by modifying the surface morphology. The lapse rates considered by the offline correction are no longer valid at the ice sheet margins. If used (1-way simulation), this correction implies an overestimation of the sea level rise contribution of 2.5 %. The mitigation of the melt lapse rate on the margins can only be corrected by using a full coupling between an ice-sheet model and an atmospheric model.

1 Introduction

The mass balance (MB) of the Greenland Ice sheet (GrIS) is a key factor of the future estimation of sea level rise (SLR) (Oppenheimer et al., 2019). Among the components of the GrIS MB, changes in Surface Mass Balance (SMB) and iceberg discharge, surface meltwater runoff appears to be the main contributor to future SLR (Goelzer et al., 2013, 2020; Enderlin et al., 2014; Choi et al., 2021).

https://doi.org/10.5194/tc-2023-15
Preprint. Discussion started: 15 February 2023

As a long-term consequence, the melting ice will also decrease the ice sheet topography. Such a thinning will influence the regional atmospheric circulation, particularly affecting the spatial distribution of precipitation (Vizcaíno et al., 2010). It will also enhance the surface melt through a positive feedback cycle since the lower elevation of the ice sheet surface results in stronger warming and melt (hereafter, melt-elevation feedback). Changes in topography are generally not considered in climate models, but they are in Ice Sheet Models (ISMs). In contrast, atmospheric models, especially Regional Climate Models (RCMs), can represent the atmospheric circulation, SMB and its components in a more realistic way than ISMs through the explicit resolution of physical polar processes involved in the interactions between the atmosphere and ice or snow surfaces. Therefore, the most optimal method to represent the melt-elevation feedback would be based on a coupling between a RCM and an ISM.

This kind of coupling has two main disadvantages. First, a RCM-ISM coupling is not trivial because the two types of models do not rely on the same spatial and temporal scales. Simulations of ice flow processes require relatively large time steps (of the order of one month) compared to those required for atmospheric dynamic resolution (of the order of one minute), which are significantly shorter. Conversely, ISMs are implemented on a finer grid (of the order of one kilometre) than RCMs (of the order of ten kilometres). These differences result in a high computational time for coupled simulations. Then depending on the ISM used in a RCM-ISM coupling, the response to climate change may be significantly different (Goelzer et al., 2013, 2020), while RCMs simulate relatively similar SMB for the same forcing (Fettweis et al., 2020). This means multiple couplings would be necessary between several ISMs and RCMs to quantify uncertainties.

An often-used alternative to coupling is to impose atmospheric conditions from an RCM on an ISM; either the ISM resolves an SMB based on the monthly mean temperature change (Robinson et al., 2011) or the SMB is directly imposed to the ISM (Goelzer et al., 2013). However, since the topography and ice mask are fixed in the RCM, this method does not consider the positive feedback between melt and elevation. In this case, it is possible to use vertical gradients as a function of local elevation variations (which implicitly takes into account the melt-elevation feedback) to correct the elevation-dependent MAR outputs for topographic variations simulated by the ISM (Franco et al., 2012; Helsen et al., 2012). ISMs can then use RCM-corrected outputs as direct inputs. This offline method is notably used in the Ice Sheet Model Intercomparison Project for CMIP6 (ISMIP6, Goelzer et al., 2020) exercise. Using an offline correction works well as long as SMB (particularly melt) is mainly influenced by the surface elevation. It could be limited once surface elevation changes affect synoptic circulation through modifications of precipitation patterns, for instance. Both methods have been compared in Le clec'h et al. (2019) by using GRISLI (ISM), and MAR (RCM) forced with MIROC5 as forcing (from CMIP5). They highlighted the need for a coupling beyond 2100 due to the melt-elevation feedback and precipitation-circulation changes that cannot be correctly represented when using a simple offline correction as soon as the topography changes become significant.

As the coupling is dependent on the used ISM, we present a new coupling between the climate model MAR and the Parallel Ice Sheet Model (PISM) following an extremely warm scenario (CESM2 SSP5-8.5) until 2200. The coupling, explicitly considering the melt-elevation feedback, is compared to an alternative method of offline correction of the SMB to consider this feedback. First, the aim is (1) to analyse what becomes GrIS in 2200 with this new coupling following an extreme scenario. By comparing our coupled simulation with the 1-way experiment, we (2) assess the offline method to represent the melt-elevation

https://doi.org/10.5194/tc-2023-15
Preprint. Discussion started: 15 February 2023

feedback. We also highlight (3) which atmospheric feedback, as well as physical processes, are influenced by the changes in surface topography.

Section 2 describes the methodology and different experiments used in the study. The first part of the result in Section 3.1 presents the GrIS evolution as simulated with our coupling until 2200. Section 3.2 compares 1-way and 2-way experiments by evidencing new negative feedback triggered by the evolving surface topography of the GrIS in the 2-way-coupling method. Results are discussed in Section 4 and we end by the conclusion in Section 5.

2 Data and methodology

2.1 Models

2.1.1 Regional climate model MAR

The MAR model is a hydrostatic regional climate model specially developed to represent polar climates. It is largely used over Greenland (Delhasse et al., 2020; Fettweis et al., 2020; Hofer et al., 2020; Fettweis et al., 2021) but also over Antarctica (Agosta et al., 2019; Kittel et al., 2020; Amory et al., 2021). The version 3.11.5 of MAR (MAR hereafter Fettweis et al., 2021) is used here at 25 km spatial resolution. For the coupling process, the important variables are SMB and surface temperature (ST), which are required as input by the ISM. These surface variables result from the interactions between the atmosphere and the first snow/ice layers of the ice sheet represented by the Surface-Ice-Snow-Vegetation-Atmosphere-Transfer (SISVAT) module in MAR. The good performance of MAR to simulate atmosphere/ice interactions (Delhasse et al., 2020) is one of the keys to a successful coupling because it determines the two input variables used by the ISM.

As MAR is a regional climate model, it needs lateral forcing fields every 6 hours to represent its own climate above the selected domain. We, therefore, selected one of the most climate-sensitive models (Hofer et al., 2020) among the CMIP6 models (CESM2) using the SSP5-8.5 scenario from the IPCC (Eyring et al., 2016; O'Neill et al., 2016; Riahi et al., 2017), and available when starting the study. The equilibrium climate sensitivity (a hypothetical value of global warming at equilibrium for a doubling of CO2 relative to a 140-year period in the pre-industrial) of CESM2 is + 5.2 °C (mean of CMIP6: + 3.2 °C, Meehl et al., 2020). This choice was motivated by the aim of representing the worst (i.e. warmer) future scenario for the GrIS, SSP5-8.5 being the most extreme scenario with an additional radiative forcing of 8.5 Wm^{-2} in 2100. The aim is to highlight the limits of both methods in representing the melt-elevation feedback in conditions of extreme warming.

CESM2 (SSP5-8.5, 6-hourly outputs) is currently only available until 2100. We extend our simulations to 2200 by forcing MAR with the last 10 years (2091 – 2100) of CESM2 sampled randomly over 2101 – 2200 (Table S1 in the Supplement). This means we apply a stabilised climate (mean conditions and interannual variability) to Greenland over 100 years. This extension of the large-scale forcing enables us to distinguish the effect of the rapidly increased warming projected with this scenario until 2100 compared to the effect of continued stable warming of + 7 °C above Greenland until 2200.

https://doi.org/10.5194/tc-2023-15
Preprint. Discussion started: 15 February 2023

2.1.2 Ice Sheet Model PISM

To represent the dynamics and surface elevation of the GrIS, we use the 3D high-resolution numerical ice-sheet/ice-shelf model Parallel Ice Sheet Model (PISMv1.2.1, called PISM hereafter, Bueler and Brown, 2009; Winkelmann et al., 2011). PISM is a polythermal and thermomechanically coupled model and includes a hybrid stress balance mode (Bueler and Brown, 2009; Aschwanden et al., 2012). The Shallow Ice Approximation (SIA) for slow-flowing ice with vertical deformation (Hutter, 1983) is combined with Shallow Shelf Approximation (SSA) for fast-flowing ice streams and shelves with longitudinal stretching (Morland et al., 1987). Basal shear stress determines the sliding velocities and is related via a power law with a Mohr-Coulomb criterion. This relates the yield stress to parametrised till material properties (friction angle) and the effective pressure of the overlying ice on the saturated till (Bueler and Van Pelt, 2015). We use a non-conserving simple hydrology model that connects the till water content to the basal melt rate (Bueler and Van Pelt, 2015). Our friction angle is altered linearly between $5°$ and $40°$ between -700 m and 700 m of bedrock elevation after Aschwanden et al. (2016). The resulting lower friction for lower altitudes and below sea level leads to an additional increase in surface velocities at the ice sheet margins, resulting in an improved match of flow structure for the glaciers. To match the present-day ice area extent, we apply a strong negative SMB at the margins of Greenland present-day ice mask. Thus only ice retreat is allowed in our experiment. Glen's flow law describes the ice rheology with the following flow law parameters: flow enhancement factor (E = 3), exponent of the sliding law (q = 0.6), and exponent of the flow law for the SSA (n = 3). All other parameters were set to default. No bedrock deformation was considered, and changes in ice-ocean interaction were neglected, as the submarine melt rates were kept constant.

2.1.3 Inisialisation of PISM

PISM is forced by yearly ST and SMB from MAR forced by CESM2. To achieve a stable spinup state, we forced PISM with the MAR mean fields (ST and SMB) over 1961 – 1990, when the GrIS was close to balance (Fettweis et al., 2017). However, for a realistic thermodynamics representation of the ice sheet, the temperature evolution of the last glacial cycle has to be considered.

Thus the first model initialisation was run over 125 000 years with a scalar temperature anomaly of the 2D-temperature mean field of 1961 – 1990. The historical time series is derived from Oxygen Isotope Records from the Greenland Ice Core Project (GRIP, Johnson et al., 2019). We followed the grid refinement defined by Aschwanden et al. (2016) for computational efficiency. Starting in SIA-only mode, and an 18 000 m grid at -125 000 years, we refined our grid to 9 000 m at -25 000 years and to 4500 m at -5000 years. For the last -1000 years, we kept the resolution fixed but added the SSA to the SIA stress regime to represent better the fast-flowing outlet glaciers.

2.2 Coupling method

The coupling between both models has been performed by exchanging yearly outputs (SMB and ST from MAR, and ice thickness from PISM) on the 1st January of each year for 1991 – 2200 as described in Le clec'h et al. (2019). For MAR, this

https://doi.org/10.5194/tc-2023-15
Preprint. Discussion started: 15 February 2023

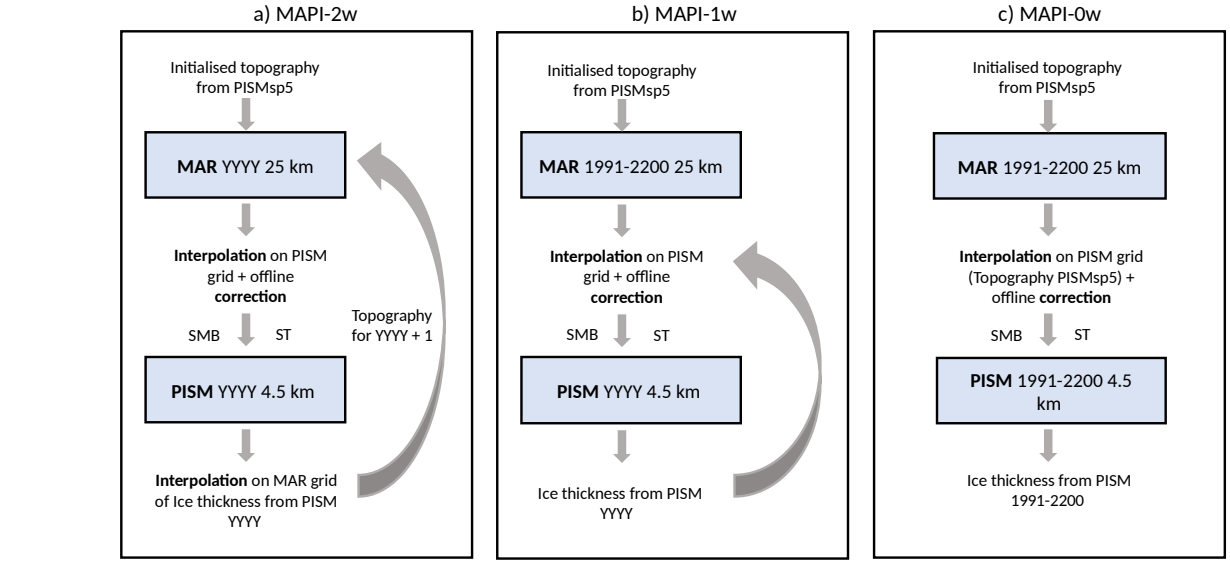

Figure 1. Coupling details for a) 2-way, b) 1-way and c) 0-way experiments.

induces updating the surface elevation and ice extent of the ice sheet at the beginning of each year with PISM results from the previous year, whereas SMB and ST are used as forcing fields for PISM.

Before any data exchange between the models, data has to be interpolated on the destination grid because the two models were run at two different spatial resolutions (25 vs 4.5 km). The surface elevation simulated by PISM is then interpolated using a four-nearest-neighbour distance-weighted method on the MAR grid at 25 km. For the MAR variables, they are interpolated using the same method on the PISM grid at 4.5 km. However, they are further corrected by considering the difference in altitude between the two grids at the time of interpolation thanks to local vertical SMB/ST gradients. This method is described in (Franco et al., 2012) and is called offline correction hereafter. This method corrects the altitude-dependent variables (such as SMB and ST) by applying a local linear gradient of the variable according to the surface elevation differences between the current MAR grid cell, and the surrounding MAR grid cells (9 grid cells considered here to compute the vertical gradient).

2.3 Simulations

2.3.1 Inisialisation of the coupling

The coupling requires initialisation to achieve an equilibrium state between the two models over a reference period (1961 – 1990). Successive forcings of each model by the other one should produce similar results to the previous iteration over the same reference period. These simulations are called spinup hereafter. In practical terms, we firstly forced PISM using the SMB and

https://doi.org/10.5194/tc-2023-15
Preprint. Discussion started: 15 February 2023

ST climatology of MAR 1961 – 1990 (MARsp0, based on the observed topography and ice mask, and CESM2 as a large-scale forcing field, Howat et al., 2014, 2017) and temperature anomalies of the last glacial cycle (see Section 2.1.3) resulting in a first equilibrium state (PISMsp1). This method assumes that the ice sheet topography before the last glacial cycle was similar to the preindustrial one and reiterates this process should correct for errors in ice thickness. The next step (MARsp1) consists in running MAR using the new ice extent and topography from PISMsp1 over the same period (still 1961 – 1990). The corrected surface topography (PISMsp1) together with the corrected SMB and ST climatology (MARsp1) are the new base to re-start our initialisation over a whole glacial cycle, as described in Section 2.1.3. The new surface topography, PISMsp2, is then used to derive the new climatological mean field of (1961 – 1990) with MAR (MARsp2). We repeated these successive forcings (5 iterations are needed here) until both models reached an equilibrium state regardless of the new forcing. This means that differences between the two spinup stages no longer influence the other model (Fig. S1 in the Supplement).

The PISMsp5 topography, the last step of the initialisation process, will be the initial state of the different simulations compared here and is used to run the MAR reference simulation over the reference period (MARref). As our projections could not be evaluated, we compared performances of MARref forced with CESM2 to MAR using the PSIMsp5 topography and forced with the observed climate, i.e. the reanalysis ERA5 here (Hersbach et al., 2020). The main point is that MARref is significantly colder than MAR forced by ERA5 in the south of Greenland, but this bias does not significantly influence SMB results (See Fig.S2 in the Supplement). It is due to the cold bias of CESM2 compared to reanalyses (Hofer et al., 2020).

The ice sheet topography and velocity field of the PISMsp5 final run and their difference to observational data sets are depicted in the Supplement (Fig. S3). The ice sheet thickness of the final spinup is overestimated up to 150 m in the northeast and southwest of the GrIS. In comparison, the northwest and central west are underestimated up to 200 m compared to the observational data set (Fig. S3a). As there is no complete observational velocity data set from 1961 to 1990, we, therefore, compare it with the complete velocity data set by Joughin et al. (2018), which gives the average velocities from 1995 to 2015. Our comparison shows a general agreement of the velocity pattern with an average difference between modelled and observed ice speeds of $\pm$ 80 $\mathrm{m\,yr^{-1}}$ on the margins (Fig. S3b). In some fast-flowing glacier regions, differences are well larger. However, the coarse resolution (4.5 km) compared to the proximity of smaller glaciers (500 m), which are solved by the observations, lead to strong deviation in their comparison.

2.3.2 Coupled simulation

The first simulation is the 2-way experiment which consists of a coupled simulation of MAR and PISM called MAPI-2w hereafter. We started to run MAR in 1991 with the PISMsp5 topography forced with CESM2 (Fig. 1a). At the end of this first year, we interpolated SMB and ST on the PISM grid with the offline correction. Then, PISM is running for the same year and produces a new ice thickness that will further be interpolated onto the MAR grid to start the following year (i.e. 1992) with an updated topography. When the MAR topography is updated, we also update the ice mask in function of PISM ice extent. The melt-elevation feedback is, therefore, explicitly taken into account by the MAPI-2w simulation through an evolving topography in MAR.

https://doi.org/10.5194/tc-2023-15
Preprint. Discussion started: 15 February 2023

2.3.3 Uncoupled simulations

The 1-way experiment (called MAPI-1w hereafter) consists in a simulation where MAR is running with PISMsp5 topography (built over the reference period) for 1991 – 2200 without any more interaction from PISM to MAR (Fig. 1b). Then we interpolated the yearly results of SMB and ST from MAR to the PISM grid with the offline correction. Thus, the new PISM input variables were corrected for changes in the surface height of the evolving ice sheet topography of PISM compared to the fixed MAR surface elevation. The MAPI-1w experiment considers then the melt-elevation feedback a posteriori through the offline correction, meaning that it is not explicitly solved by any of the two models (MAR or PISM), nor are the implied physical processes. As MAR is evolving alone, no update on the ice mask has been done. To be consistent, we consider the smallest ice mask all along the analyses, meaning the one in 2200 of the MAPI-2w simulation, to compare both simulations.

We also consider a PISM simulation forced with MAR-fixed-topography corrected over the initial PISM topography (PISMsp5). This experiment is called the MAPI-0w experiment (Fig. 1c) hereafter due to its non-consideration of the melt-elevation feedback.

2.4 Representation of the results

For the sake of consistency of the results, we decided to present all results on the PISM grid, whether they are PISM or MAR outputs. The MAR variables used in the analyses below are therefore interpolated on the PISM grid. While those from the coupled simulation explicitly include the influence of melt-elevation feedback, the variables from the uncoupled simulation (MAPI-1w) are corrected offline during the interpolation. This correction is applied to the variables dependent on the surface elevation influence, i.e., temperature, SMB, meltwater production and runoff. On the other hand, the following variables will not be corrected during their interpolation since they do not depend on the evolution of the surface elevation: total precipitation (snowfall and rainfall) and wind. However, some comparisons have been carried out on the MAR grid, but this is well specified each time.

The two main PISM simulations, which are compared hereafter (MAPI-2w and -1w), evolve independently and consequently have differences in surface topography. These differences (Fig. S4 in the Supplement) are only responsible for 10 % of the MB differences between two experiments in 2200 (Fig. S5 in the Supplement) and will be further neglected. Throughout the analysis, we will consider the MAR results interpolated on the MAPI-2w coupled PISM grid (4.5 km) regardless if they are from MAR coupled or uncoupled simulation.

3 Results

3.1 Coupled (S)MB

This section is exclusively dedicated to describing changes in (surface) mass balance and their components in the future as simulated with the 2w-coupling experiment compared to the reference period.

https://doi.org/10.5194/tc-2023-15
Preprint. Discussion started: 15 February 2023

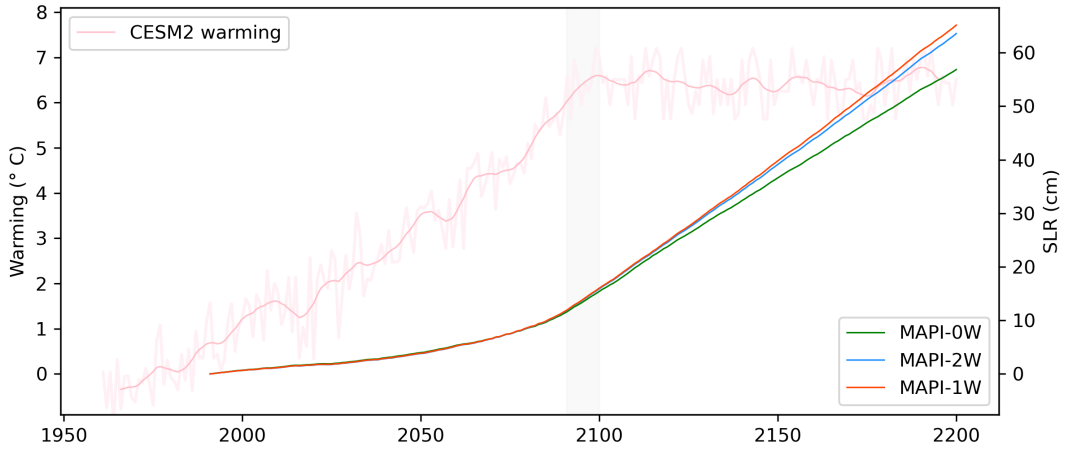

Figure 2. Contribution to sea level rise (SLR, cm) of the Greenland Ice Sheet according to MAR-PISM 2-way (in blue),) 1-way (in red) and 0-way (in green) experiments. In pink is the corresponding warming (°C) applied in the MAR lateral boundaries following CESM2 SSP5-8.5 (mean temperature at 600 hPa over Greenland). The last 10 years of CESM2 randomly sampled until 2200 to extend the CESM2-forcing of MAR are in grey.

Our results project a fast increase in annual mass loss for an extreme warming rate (Fig. 2). It corresponds to a contribution to sea level rise of 16 cm in 2100 (< -50 $\mathrm{Gt.10^{-3}}$) for a global warming of + 7 °C in 2100 (+ 6.8 °C on average for 2091 – 2100) compared to our reference period (1961 – 1990). After 2100 this warming is stabilised (+ 7 °C on average for 2101-2200), the ice sheet continues to lose mass, and the sea level rise contribution reaches 64 cm (< -200 $\mathrm{Gt.10^{-3}}$). Since there is an acceleration of the mass loss just before 2100, even with a stabilised climate, mass loss is not stabilised in 2200.

Whereas the GrIS is retreating by a few kilometres all around its margins (Fig. 3), extremely negative cumulated mass balance (MB) in 2200 results in a decrease in surface elevation of several hundred metres at the GrIS margins. The western margin is more affected by the mass loss and, thus, the decrease in elevation. Many peripheral glaciers seem to disappear by 2200, especially in the east and north of the island.

The SMB decrease largely drives the increase in mass loss. To attribute the individual factors of the SMB loss, we examine the native 25 km output MAR-2w (Fig. 4 solid lines). The SMB evolution is marked by an accelerated decrease after 2050 to 2100 and a slowdown from 2100 to 2200 when the climate stabilises again. The changes in SMB are dominated by meltwater runoff (RU hereafter) resulting from larger meltwater production (ME hereafter) not refreezing into the snowpack.

Due to global warming, we expect more precipitation. Combined with the lower surface elevation, we also expect more liquid precipitation. The snowfall (SF) evolution remains constant until the end of the simulation (Fig. 4). The slight increase in total precipitation is mainly due to increased rainfall (RF). Surprisingly, only a short part of RF increase (1 % when comparing RF

https://doi.org/10.5194/tc-2023-15
Preprint. Discussion started: 15 February 2023

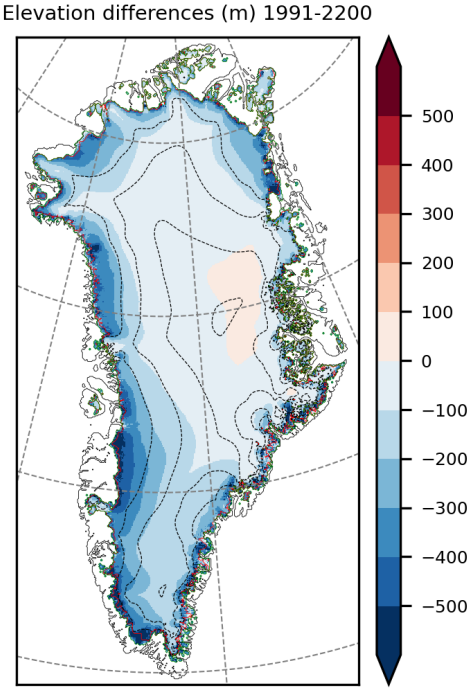

Figure 3. Surface elevation changes (m) as simulated by the 2-way coupling between MAR and PISM between 1991 and 2200. In green, the ice extent as in 1991 and in red as in 2200.

from MAR coupled, solid lines, and uncoupled, dashed lines) is caused by the decrease in surface elevation, which converts more SF into RF.

The spatial distribution of the SMB component changes is explained mainly by the warming of the scenario and emphasised by the decrease in surface elevation until 2200 (Fig. 5a). ME and RU (Fig. 5e and f), which drive the spatial pattern of the SMB (Fig. 5d), are projected to occur more inland. For instance, almost the entire southern half of Greenland is affected by RU in 2200. This results in a SMB decrease in these regions triggering changes in surface topography, evidencing the dependence of the MB on the SMB.

While total precipitation over Greenland does not appear to change significantly (Fig. 4), its spatial distribution does change with topography compared to the reference period in the coupled simulation. There is a significant decrease in total precipitation (SF + RF, Fig. 5c) over the southeast due to synoptic features of the large-scale forcing (CESM2, not shown). Conversely, our simulation projects significantly increase over the west and north of Greenland. The increase in the west is a consequence of the ice sheet thinning as clouds can penetrate more inland due to a weaker topographic barrier effect and a delayed condensation due to further lift-up of air masses. We attribute changes in snowfall for the north of Greenland to more humidity content associated with atmospheric warming, as this region is particularly dry and cold over present-day conditions. This results in a slight increase when integrating the precipitation over the whole ice sheet, mainly due to an increase in RF resulting from

https://doi.org/10.5194/tc-2023-15
Preprint. Discussion started: 15 February 2023

The Cryosphere
Discussions
Open Access
EGU

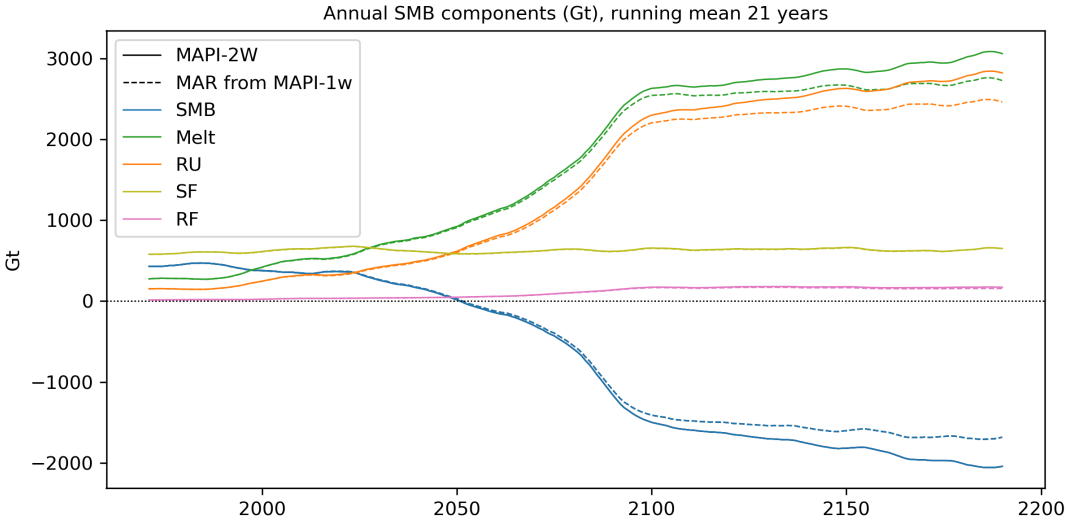

Figure 4. Surface mass balance (SMB, in blue), Meltwater production (ME, in green), meltwater Runoff (RU, in green), Snowfall (SF in yellow) and Rainfall (RF, in pink) evolution (in Gt) as simulated by MAR 2-way coupled with PISM (MAPI-2w) from 1991 to 2200. Dotted lines are corresponding evolution as simulated by MAR uncoupled (MAPI-1w).

global warming and changes in surface elevation, as explained before. However, significant changes in the spatial distribution of precipitation do not influence the global pattern of SMB since runoff changes are far larger.

The decreased mass loss of the ice sheet is accompanied by an overall speedup of the ice dynamics inland and a slow down at the margins (Fig. 6a). Surface velocity relates to the driving stress, and the spatial pattern of driving stress changes (Fig. 6b) mainly explains the spatial pattern of changes in surface velocities. As the driving stress relates to the product of ice thickness and surface slope, the pronounced thinning at the margins of the ice explains the reduction in driving stress in these regions. While there is also an increase in surface slope at the margins, which would increase the driving stress, the thinning is of larger importance and determines the reduction in driving stress. Although less pronounced than in the margins, the ice interior still experiences an increase in surface slope. Further inland, the increase in surface slope emphasises the driving stress as the thinning is smaller than the thinning at the margins. Therefore the increased driving stress leads there to higher surface velocities.

The overall pattern of speedup in the ice interior and slow down at the margins is observed in the 2-way and 1-way experiments. However, in MAPI-2w, ice thickness is slightly larger at the margins and thinner in the ice interior than in MAPI-1w. At the margins, this reduces the surface slope and, compared to the 1-way experiment, leads to slower velocities (Fig. S4b in the Supplement).

https://doi.org/10.5194/tc-2023-15
Preprint. Discussion started: 15 February 2023

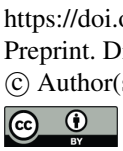

The Cryosphere
Discussions
Open Access
EGU

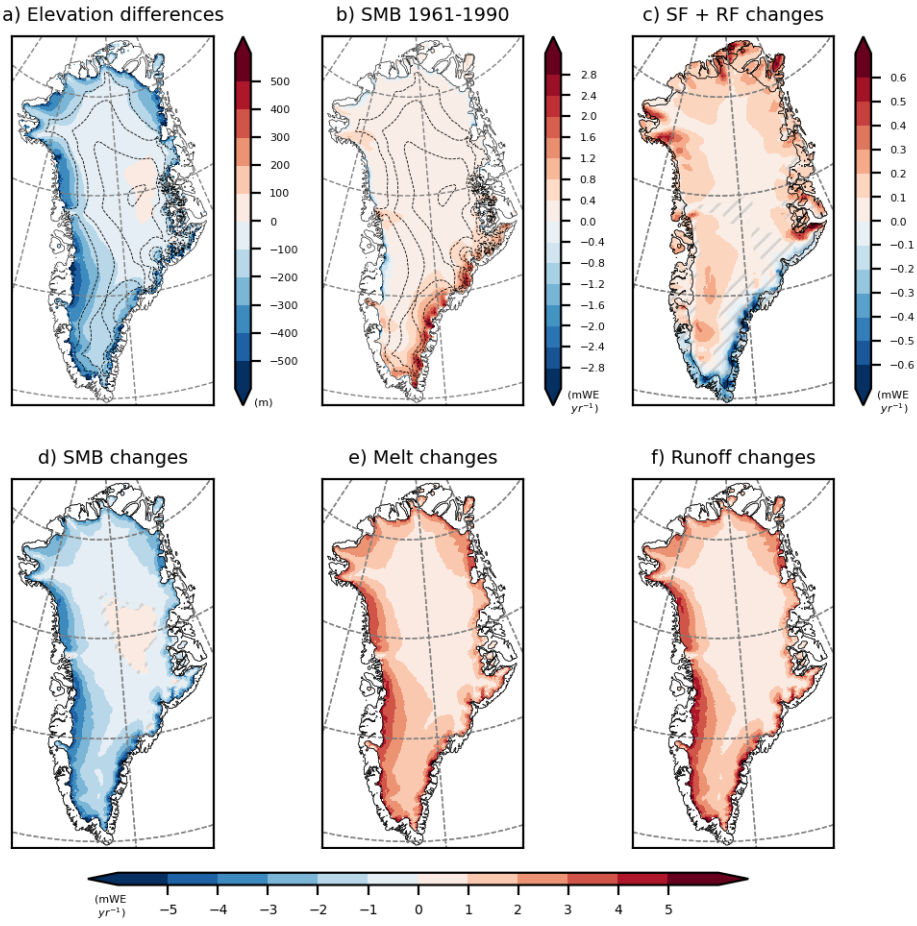

Figure 5. a) Surface elevation changes (m) between 1991 and 2200 as simulated by the MAR-PISM 2-way coupling (MAPI-2w). b) Surface mass balance (SMB, mWE yr^{-1}) for the reference period (1961 – 1990) as simulated by MAPI-2w. c) Precipitation (snowfall, SF and rainfall, RF, mWE yr^{-1}), d) SMB (mWE yr^{-1}), e) Meltwater production (mWE yr^{-1}) and f) meltwater Runoff (mWE yr^{-1}) changes in 2171 – 2200 compared to the reference period. Insignificant changes are hatched (smaller than the interannual variability of the reference period).

3.2 Comparison of coupled and uncoupled experiments

This section focuses on the differences in the results obtained by the two methods of considering the melt-elevation feedback (MAPI-1w vs MAPI-2w).

Comparing the total mass loss in 2200 (Fig. 2), the different strategies in representing the melt-elevation feedback (MAPI-1w vs MAPI-2w) do not result in a significantly-different total mass loss in 2200. Total ice loss is 229 x10^3 Gt with MAPI-2w and 234 x10^3 Gt with MAPI-1w, meaning that MAPI-1w overestimates the SLR contribution of 2.5 % (1.6 cm) compared to MAPI-2w. MAPI-0w largely underestimated ice loss by 10.5 % (6.7 cm less of SLR than MAPI-2w) due to its non-representation of the melt-elevation feedback. These three experiments start to diverge when the climate is stabilised.

https://doi.org/10.5194/tc-2023-15
Preprint. Discussion started: 15 February 2023

The Cryosphere
Discussions
Open Access
EGU

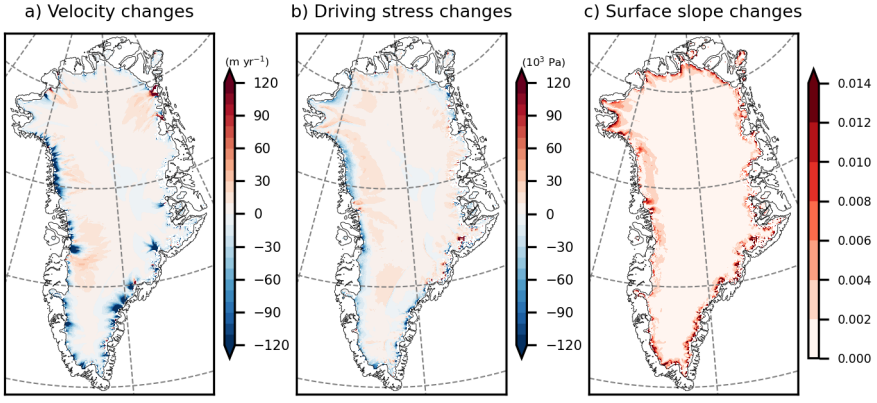

Figure 6. Changes (2200 – 1990) in a) velocity (m yr^{-1}), b) driving stress (10^3 Pa) and c) surface slope of the coupled MAR-PISM simulation (MAPI-2w).

The MB overestimation by MAPI-1w is contrary to the result of the MAR outputs, where MAPI-2w gave higher melt rates than MAPI-1w (Fig. 4 solid vs dashed lines). This highlights that when we correct the SMB for melt-elevation feedback by the offline correction (MAPI-1w on PISM grid), the SMB become exaggeratedly negative compared to the 2-way coupling, which explicitly considers this feedback. It is in opposition to (Le clec'h et al., 2019) as discussed later.

The corrected SMB provided to PISM in both MAPI-1w and MAPI-2w (Fig. 7) differ significantly at the margin of the ice sheet, indicating a greater mass loss for MAPI-1w. The different SMB components are analysed here (Fig. 7) to identify what causes this underestimation of the MAPI-1w-corrected SMB. Firstly, whether on the east or west coast, there is a different distribution of total precipitation when simulated by MAPI-2w compared to MAPI-1w (Fig. 7f). Precipitation falls more inland (positive differences) in the coupled mode since the slope is flattened, but this is not significant compared to the annual variability (2171 – 2200 standard deviation). Therefore, this does not explain the SMB differences in the margins between the two simulations. The main driver is the meltwater runoff (Fig. 7b) resulting from the ME excess (Fig. 7e) not refreeze in the snowpack. ME depends on the sensible heat flux (SHF) related to air temperature and wind speed which are also overestimated on the margins by MAPI-1w (Fig. 7d and e).

The underestimation of SMB in MAPI-1w is due to an overestimation of the melt-elevation feedback by the offline correction when interpolating MAPI-1w towards the PISM grid compared to the explicit consideration of this feedback in MAPI-2w. This correction is based on the linear temperature dependence with the surface elevation to account for the melt-elevation feedback that alters the SMB and related variables. The correction applies local linear gradients according to these altitude differences. We compare, on the MAR grid, the yearly evolution of the altitude differences between the two experiments (coupled and uncoupled) with the evolution of the temperature differences inside the ice sheet and on the margin (Fig. 8a). We notice that on the margin, the dependence is no longer linear (analyse for different other grid cells have been carried out but are not shown here). Inside the ice sheet, the temperature-elevation relation, evaluated as -0.4 °C/100m, remains linear. In our example, modifications of the topography in the 2-way coupling experiment have modified this linear relationship to -0.1 °C/100m of

https://doi.org/10.5194/tc-2023-15
Preprint. Discussion started: 15 February 2023

The Cryosphere Discussions
Open Access
EGU

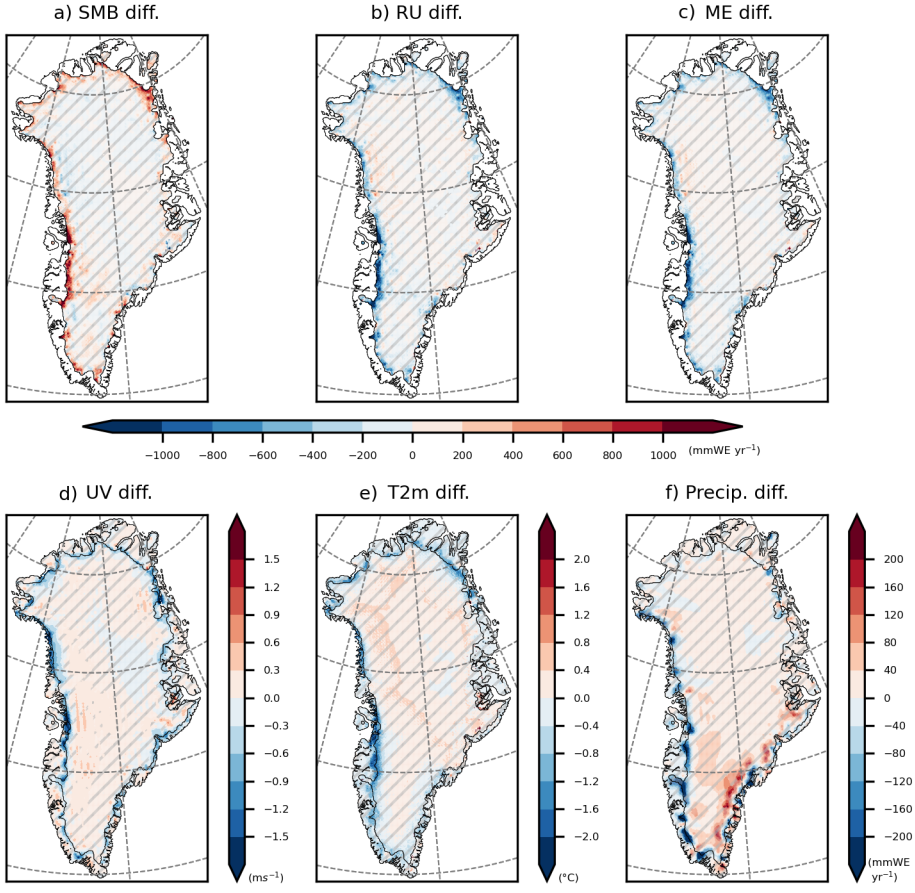

Figure 7. Differences (2w minus 1w) of a) SMB (mmWE yr^{-1}), b) Runoff (RU, mmWE yr^{-1}), c) meltwater production (ME, mmWE yr^{-1}), d) 10m-wind speed (UV, ms^{-1}), e) 2m-temperature (T2m, °C), and f) total precipitation (Precip. are the sum of rainfall and snowfall) between the MAPI-2w and MAPI-1w simulations for 2171 – 2200. Insignificant differences are hatched (smaller than the interannual variability of 2171-2200).

the temperature increase with the surface elevation lowering along the margins. The same relationship is illustrated for melt differences (Fig. 8b), confirming the modification in linear dependence with changes in surface elevation. This highlights two main elements: (1) the linear-offline correction of SMB is no longer valid in the ice sheet margins; (2) the non-linear relationship between temperature and altitude driving the melt-elevation feedback lead to mitigation of this feedback along the ice sheet margins.

The mitigation of the melt-elevation feedback in the MAR-coupled simulation is explained by the modification of the local atmospheric circulation on the margins around the GrIS. The evolution of the topography in the coupled simulation (for instance, Fig. 9e) causes a decrease in the melt increase with the elevation lowering. As meltwater production depends on the

https://doi.org/10.5194/tc-2023-15
Preprint. Discussion started: 15 February 2023

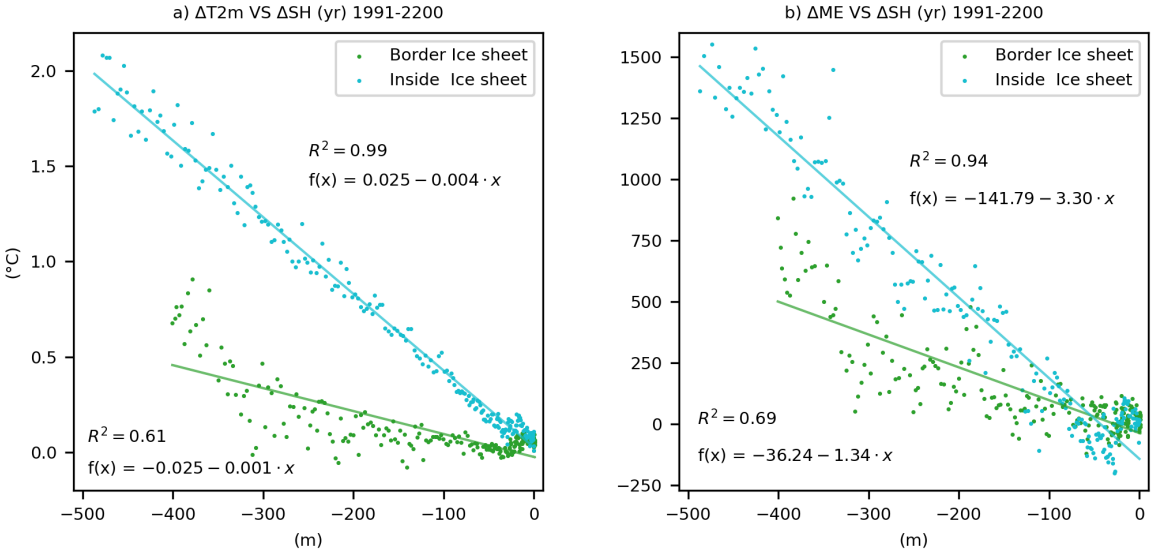

Figure 8. Association of the yearly (1991 – 2200) differences on MAR grid in surface elevation (ΔSH, m) with a) differences in 2m-temperature (ΔT2m, °C) and b) meltwater production (ΔME, mmWE yr^{-1}) between coupled (MAPI-2w) and uncoupled (MAPI-1w) simulation for a MAR grid cell (25 km) inside the ice sheet (49.26 ° W, 67.05 ° N, in blue) and one at the boundary with the tundra (48.83 ° W, 67.05 ° N in green). These grid cells are located on the same section of the West Greenland than in Fig. 9. Regressions are presented in the respective colours.

near-surface temperature and the wind through the sensible heat flux, we compare the vertical temperature and wind speed patterns above both simulation topographies along a transect crossing the ice sheet. The example illustrated in Fig. 9 highlights that the north-south wind component (v-wind, positive northward) is larger in the uncoupled simulation on the grid cell at the margin of the ice sheet (inside the ice sheet, Fig. 9c and d). Secondly, the mean near-surface temperature that appears on the 2200-topography (coupled MAR) on the same grid-cell of the ice sheet margin is lower than the temperature computed on the uncoupled MAR topography while at lower altitude (Fig. 9a and b). Mitigation of the wind and the temperature in the MAR-coupled simulation explains the weaker melt increase with elevation lowering. It cannot be directly illustrated because the differences between coupled and uncoupled MAR melt on the MAR grid remain dominated by the melt-elevation feedback influence.

Temperature changes and (v)-wind speed decrease in coupled MAR simulation compared to uncoupled one can be explained by mitigation of the barrier wind impact on the surface melt. Barrier winds occur when air masses from the tundra cross the ice sheet, which acts as an orographic barrier (Van den Broeke and Gallée, 1996). These winds induce warm air advection from the tundra (warmer than the surrounding air of the ice sheet) locked by the orographic barrier and leading to northward wind (on the west coast) along the ice sheet margin. They are associated with high melt events due to increased wind speed and positive temperature along the ice sheet margins. Considering the changes in topography in MAPI-2w compared to MAPI-

https://doi.org/10.5194/tc-2023-15
Preprint. Discussion started: 15 February 2023

The Cryosphere Discussions
Open Access
EGU

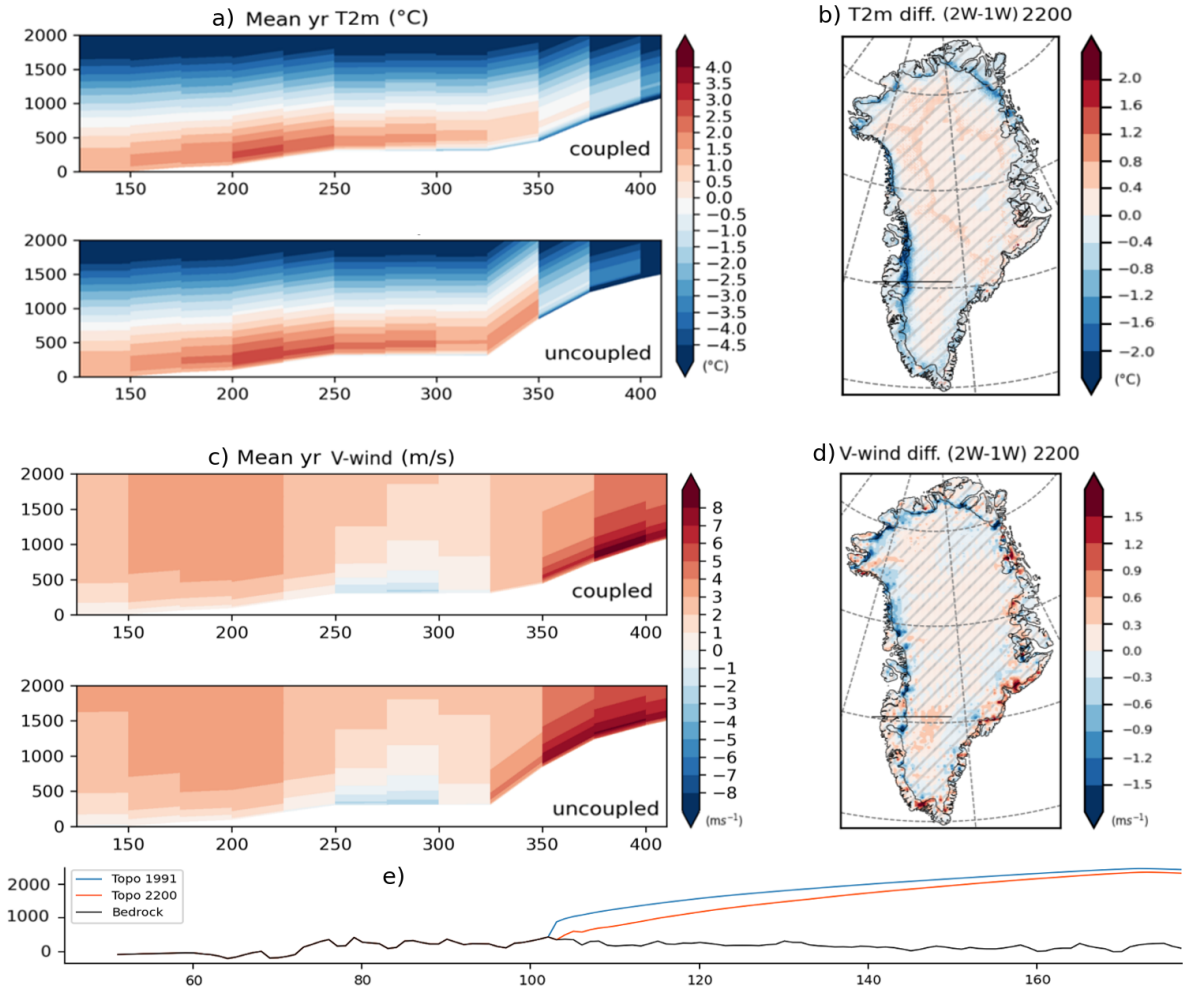

Figure 9. Cross sections along 66.64–67.35 ° N of a) temperature (T2m, °C) and c) V-wind component (north-south, ms^{-1}) on the MAR grid for the coupled (above) and the uncoupled (below) simulation. Differences in b) 2m-temperature (°C) and d) V-wind component (ms^{-1}) between 2-way and 1-way experiments of MAR and PISM (MAPI-2w - MAPI-1w) in 2200. Non-significant differences (lower than the interannual variability over 2171 – 2200) are hatched. T2m and V-wind are interpolated in PISM grid (b and d) to be consistent with other figures, T2m is corrected with the offline correction but not the V-wind as it is not related to surface elevation. e) Cross section along black lines in b) and d) on the west coast of the PISM grid (similar to the cross-section in a) and c) subplots) on MAR grid 66.64–67.35 ° N) of the surface elevation (m) of the MAPI-2w in 2200 (in red), in 1991 in blue (fixed topography in MAR for MAPI-1w simulation) and the bedrock in black.

1w, the orographic barrier is weakened by the thinning and retreat of the ice sheet (Fig. 9e), as well as the associated barrier winds. This explains, on the one hand, why we observe a decrease in the v-wind component (north-south) in the coupled

https://doi.org/10.5194/tc-2023-15
Preprint. Discussion started: 15 February 2023

experiment. And on the other hand, it explains differences in temperature between both experiments because the MAPI-2w ice sheet experiences less warm air advection associated to barrier wind. Finally, this impacts the local gradient of melt/temperature with surface elevation.

4 Discussion

The feedback between topography and local atmospheric circulation highlighted here adds uncertainty to the SLR projections, which are already affected by uncertainties related to the ice dynamics modelling. For instance, in ISMIP6, SLR estimations vary from 6.5 to 13.5 cm in 2100 for the same climate forcing (MAR forced by MIROC5 using the RCP8.5 scenario) with the different ISMs and experiments (Goelzer et al., 2020). ISMIP6 experiments can be compared to our MAPI-1w simulation because their methodology uses MAR outputs corrected offline of the melt-elevation feedback. Such a method could be compromised to extend simulations due to uncertainties added by the varying topography of the ice sheet and its interaction with the near-surface climate discussed in this study.

Le clec'h et al. (2019) present the closest methodology of coupling to ours. They used MAR and GRISLI to represent GrIS until 2150. Besides the ISM used, the main difference in their study is the large-scale forcing field to force MAR (i.e. MIROC5, a CMIP5 model using the RCP8.5 scenario). As the future climate of MIROC5 is not as warm as CESM2 (difference of $+1.5\,^{\circ}\mathrm{C}$, Hofer et al., 2020), SLR contributions are consequently well higher by using CESM2. The 2100 warming of MIROC5 is already reached in 2080 for CESM2. Concerning their 2-way coupled simulation, given the difference in warming applied to the coupling (MIROC5 RCP8.5 vs CESM2 SSP5-8.5), their MB results in 2100 are similar to those of MAPI-2w in 2080. From the dynamical point of view, the overall pattern of speedup in the ice interior and slowdown at the margins of the GrIS towards the end of the simulation is as well observed in their study as in ours.

However, after 2100 they used constant MAR outputs (SMB and ST) to force GRISLI and extend their 1-way simulation until 2150 without continuing to run MAR on the fixed topography. By doing this, they assume that with a stable climate (no more warming), SMB becomes directly stable. To extend our MAPI-1w simulation beyond 2100, we decided to repeat the last 10 years of large-scale forcing randomly to run MAR until 2200 to allow time for snowpack to stabilise with the new warm stabilised climate over 2101 – 2200. The main difference with Le clec'h et al. (2019) is that after 2100, our MAR simulations using a fixed topography were still running with repeated CESM2 forcing fields. In contrast, in their corresponding simulation, MAR did not run beyond 2100. We compare our 1-way and 2-way experiment results with a simulation where the last 10 years of MAR from MAPI-1w outputs (same 10-years as CESM2-repeated ones) were directly used to force PISM and extend MAPI-1w simulation from 2100 until 2200 without running MAR anymore (SMB outputs 2091 – 2100 repeated, similar to the Le clec'h et al. (2019) method of the 1-way experiment). It appears that in MAPI-1w, SMB is well decreasing for decades compared to repeated MAR-fixed outputs (Fig. 10). This demonstrates that even without additional warming, the ablation area is still growing after 2100. The snowpack transforms from an accumulation to an ablation state in a larger part of the ice sheet. It needs decades to be stabilised before reaching a stable state of meltwater retention capacity. As shown in the RetMIP exercise (Retention Model Intercomparison Vandecrux et al., 2020), the required time to stabilise the meltwater retention capacity is

https://doi.org/10.5194/tc-2023-15
Preprint. Discussion started: 15 February 2023

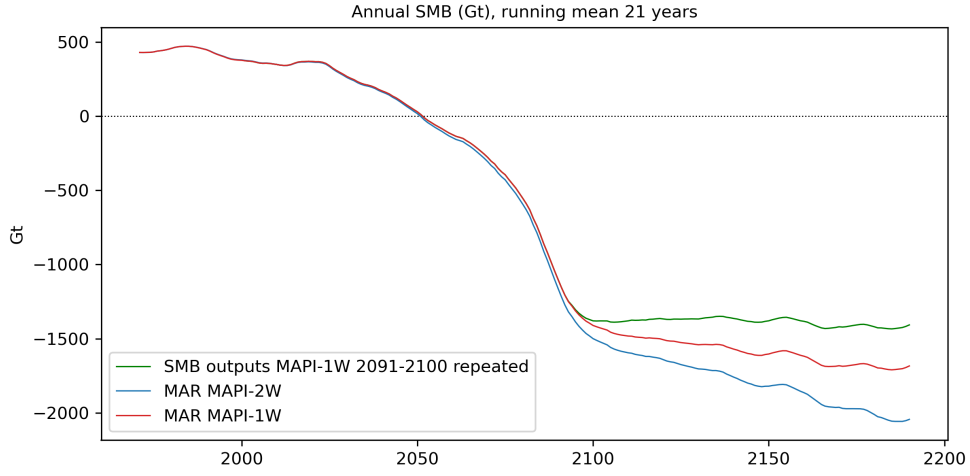

Figure 10. Yearly surface mass balance (SMB) integrated over all the ice sheet as simulated by MAR uncoupled (no update of the topography, in red), by MAR coupled (topography updated each year, in blue) and by MAR uncoupled until 2100 and last 10 years of SMB outputs repeated until 2200 (in green).

very likely model-dependent due to parameters such as the maximum liquid water enabled in the snowpack and the considered-snowpack height. This study also highlights that SMB (through runoff) cannot be considered stable as soon as the warming is stopped. During the snowpack response time, the meltwater saturates deep layers, and it becomes warmer and denser, leading to a decrease in its capacity to retain meltwater. When the snowpack reaches its maximum retention capacity, it transforms into impermeable firn or bare ice. Due to the method used in extending the 1-way simulation, this process is neglected in Le clec'h et al. (2019). Our respective comparison of the method to represent the melt-elevation feedback (1-way VS 2-way coupling) is then not comparable, as it does not have a common physical basis.

5 Conclusions

The coupling of the RCM MAR and the ISM PISM is presented here following the SSP5-8.5 scenario as simulated by CESM2. The 2-way coupling is compared to a 1-way and a 0-way (uncoupled) experiment to evaluate the importance of the melt-elevation feedback.

The first aim was to study what became GrIS in 2200 by applying such extreme conditions. Our coupling simulation projects a contribution of 64 cm to SLR by 2200 with a stabilised climate since 2100 of + 7 °C compared to our reference period (1961 – 1990). Until 2100 our results are comparable with results obtained in other studies (e.g., Goelzer et al., 2020).

The best way to represent melt-elevation feedback is the full coupling between an atmospheric model and an ice sheet model. Do not consider this feedback leads to underestimating the SLR contribution projection of 10.5. %. When comparing both methods to consider the melt-elevation feedback (coupling and offline correction), we highlight an underestimation of the

https://doi.org/10.5194/tc-2023-15
Preprint. Discussion started: 15 February 2023

corrected SMB from MAR when interpolated on the PISM grid with this correction (2.5 % of the coupled-SMB). The offline correction is no longer valid on the ice sheet margins because it does not consider mitigation of temperature increase and thus of melt due to changes in topography such as retreat and changing slope. These changes affect the wind regime in the margins of the MAR-coupled simulation. Barrier winds usually act along the ice sheet, bringing warmer air from the tundra, enhancing the surface melt and increasing the northward wind speed along the west side, for example. The key element for forming this kind of wind is the orographic barrier which is reduced with the evolving topography in MAPI-2w. Consequently, the enhanced melt is mitigated as well as melt-elevation feedback. Nevertheless, it would be necessary to analyse further the current recurrence of these barrier wind events, their characteristics and the synoptic situations favourable to their development to better identify them in the projections and to analyse their sensitivity to changes in surface topography. We concluded that coupling is needed to update the surface topography in the RCM to consider all interactions between the near-surface atmosphere and the new morphology.

By extending our simulations after the available period of large-scale forcing of MAR (CESM2), we also highlighted that it is not possible to assume that SMB is stable when climate conditions become stable. The response time of the snowpack to such warming rates and its capacity to retain meltwater have to be considered. Further sensibility tests are needed to determine if the response time of the ice sheet for stabilising the snowpack depends on the parameterisation of snow layer conditions, such as maximum liquid water content in a layer or the considered height of the snowpack simulated by the model.

In conclusion, we highlight the importance of topography in the local atmospheric circulation through the influence on wind regimes along the ice sheet margins beside the well-known melt-elevation feedback. As these processes influence melt oppositely, melt-elevation feedback is mitigated by the evolving topography. This is not considered by the offline correction often used to avoid a coupling, computationally time-consuming, between climate and ice sheet models to perform MB projections and to consider the melt-elevation feedback. Not considering this negative feedback results in an overestimation of 2.5 % (1.6 cm) of the SLR contribution compared to the full coupling results. This adds uncertainty to projections (e.g. ISMIP project) that do not consider this process, which an atmosphere-dynamics coupling can represent.

Author contributions. AD and JB conceived the study. AD and JB performed the simulations. AD led the writing of the manuscript. AD, JB, CK and XF discussed the results. All co-authors revised and contributed to the editing of the manuscript.

Competing interests. The authors have the following competing interests: Xavier Fettweis is an editor of The Cryosphere.

https://doi.org/10.5194/tc-2023-15
Preprint. Discussion started: 15 February 2023

References

Agosta, C., Amory, C., Kittel, C., Orsi, A., Favier, V., Gallée, H., van den Broeke, M. R., Lenaerts, J., van Wessem, J. M., van de Berg, W. J., and Fettweis, X.: Estimation of the Antarctic surface mass balance using the regional climate model MAR (1979-2015) and identification of dominant processes, The Cryosphere, 13, 281–296, https://doi.org/10.5194/tc-13-281-2019, 2019.

Amory, C., Kittel, C., Le Toumelin, L., Agosta, C., Delhasse, A., Favier, V., and Fettweis, X.: Performance of MAR (v3. 11) in simulating the drifting-snow climate and surface mass balance of Adélie Land, East Antarctica, Geoscientific Model Development, 14, 3487–3510, https://doi.org/10.5194/gmd-14-3487-2021, 2021.

Aschwanden, A., Bueler, E., Khroulev, C., and Blatter, H.: An enthalpy formulation for glaciers and ice sheets, Journal of Glaciology, 58, 441–457, https://doi.org/10.3189/2012JoG11J088, 2012.

Aschwanden, A., Fahnestock, M. A., and Truffer, M.: Complex Greenland outlet glacier flow captured, Nature Communications, 7, 10 524, https://doi.org/10.1038/ncomms10524, 2016.

Bueler, E. and Brown, J.: Shallow shelf approximation as a "sliding law" in a thermomechanically coupled ice sheet model, Journal of Geophysical Research: Solid Earth, 114, 1–21, https://doi.org/10.1029/2008JF001179, 2009.

Bueler, E. and Van Pelt, W.: Mass-conserving subglacial hydrology in the Parallel Ice Sheet Model version 0.6, Geoscientific Model Development, 8, 1613–1635, https://doi.org/10.5194/gmd-8-1613-2015, 2015.

Choi, Y., Morlighem, M., Rignot, E., and Wood, M.: Ice dynamics will remain a primary driver of Greenland ice sheet mass loss over the next century, Communications Earth & Environment, pp. 1–9, https://doi.org/10.1038/s43247-021-00092-z, 2021.

Delhasse, A., Christoph, K., Amory, C., Hofer, S., and Fettweis, X.: Brief communication: Interest of a regional climate model against ERA5 to simulate the near-surface climate of the Greenland ice sheet, The Cryosphere, 137, 957–965, https://doi.org/10.5194/tc-14-957-2020, 2020.

Enderlin, E. M., Howat, I. M., Jeong, S., Noh, M. J., Van Angelen, J. H., and Van Den Broeke, M. R.: An improved mass budget for the Greenland ice sheet, Geophysical Research Letters, 41, 866–872, https://doi.org/10.1002/2013GL059010, 2014.

Eyring, V., Bony, S., Meehl, G. A., Senior, C. A., Stevens, B., Stouffer, R. J., and Taylor, K. E.: Overview of the Coupled Model Intercomparison Project Phase 6 (CMIP6) experimental design and organization, Geoscientific Model Development, 9, 1937–1958, https://doi.org/10.5194/gmd-9-1937-2016, 2016.

Fettweis, X., Box, J., Agosta, C., Amory, C., Kittel, C., Lang, C., van As, D., Machguth, H., and Gallée, H.: Reconstructions of the 1900–2015 Greenland ice sheet surface mass balance using the regional climate MAR model, The Cryosphere, 11, 1015–1033, https://doi.org/10.5194/tc-11-1015-2017, 2017.

Fettweis, X., Hofer, S., Krebs-Kanzow, U., Amory, C., Aoki, T., Berends, C. J., Born, A., Box, J. E., Delhasse, A., Fujita, K., Gierz, P., Goelzer, H., Hanna, E., Hashimoto, A., Huybrechts, P., Kapsch, M.-L., King, M. D., Kittel, C., Lang, C., Langen, P. L., Lenaerts, J. T. M., Liston, G. E., Lohmann, G., Mernild, S. H., Mikolajewicz, U., Modali, K., Mottram, R. H., Niwano, M., Noël, B., Ryan, J. C., Smith, A., Streffing, J., Tedesco, M., van de Berg, W. J., van den Broeke, M., van de Wal, R. S. W., van Kampenhout, L., Wilton, D., Wouters, B., Ziemen, F., and Zolles, T.: GrSMBMIP: intercomparison of the modelled 1980–2012 surface mass balance over the Greenland Ice Sheet, The Cryosphere, 14, 3935–3958, https://doi.org/10.5194/tc-14-3935-2020, 2020.

Fettweis, X., Hofer, S., Séférian, R., Amory, C., Delhasse, A., Doutreloup, S., Kittel, C., Lang, C., Van Bever, J., Veillon, F., and Ivrine, P.: Brief communication: Reduction in the future Greenland ice sheet surface melt with the help of solar geoengineering, The Cryosphere, 15, 3013–3019, https://doi.org/10.5194/tc-15-3013-2021, 2021.

Franco, B., Fettweis, X., Lang, C., and Erpicum, M.: Impact of spatial resolution on the modelling of the Greenland ice sheet surface mass balance between 1990–2010, using the regional climate model MAR, The Cryosphere, 6, 695–711, https://doi.org/10.5194/tc-6-695-2012, 2012.

Goelzer, H., Huybrechts, P., Fürst, J. J., Nick, F. M., Andersen, M. L., Edwards, T. L., Fettweis, X., Payne, A. J., and Shannon, S.: Sensitivity of Greenland ice sheet projections to model formulations, Journal of Glaciology, 59, 733–749, https://doi.org/10.3189/2013JoG12J182, 2013.

Goelzer, H., Nowicki, S., Payne, A., Larour, E., Seroussi, H., Lipscomb, W. H., Gregory, J., Abe-Ouchi, A., Shepherd, A., Simon, E., Agosta, C., Alexander, P., Aschwanden, A., Barthel, A., Calov, R., Chambers, C., Choi, Y., Cuzzone, J., Dumas, C., Edwards, T., Felikson, D., Fettweis, X., Golledge, N. R., Greve, R., Humbert, A., Huybrechts, P., Le Clec'H, S., Lee, V., Leguy, G., Little, C., Lowry, D., Morlighem, M., Nias, I., Quiquet, A., Rückamp, M., Schlegel, N. J., Slater, D. A., Smith, R., Straneo, F., Tarasov, L., Van De Wal, R., and Van Den Broeke, M.: The future sea-level contribution of the Greenland ice sheet: A multi-model ensemble study of ISMIP6, The Cryosphere, 14, 3071–3096, https://doi.org/10.5194/tc-14-3071-2020, 2020.

Helsen, M. M., Van De Wal, R. S. W., Van Den Broeke, M. R., Van De Berg, W. J., and Oerlemans, J.: Coupling of climate models and ice sheet models by surface mass balance gradients: Application to the Greenland Ice Sheet, The Cryosphere, 6, 255–272, https://doi.org/10.5194/tc-6-255-2012, 2012.

Hersbach, H., Bell, B., Berrisford, P., Hirahara, S., Horányi, A., Muñoz-Sabater, J., Nicolas, J., Peubey, C., Radu, R., Schepers, D., Simmons, A., Soci, C., Abdalla, S., Abellan, X., Balsamo, G., Bechtold, P., Biavati, G., Bidlot, J., Bonavita, M., De Chiara, G., Dahlgren, P., Dee, D., Diamantakis, M., Dragani, R., Flemming, J., Forbes, R., FUentes, M., Geer, A., Haimberger, L., Healy, S., Hogan, R. J., Hólm, E., Janisková, M., Keeley, S., Laloyaux, P., Lopez, P., Lupu, C., Radnoti, G., De Rosnay, P., Rorum, I., Vamborg, F., Vollaume, S., and Thépaut, J.-N.: The ERA5 global reanalysis, Quarterly Journal of the Royal Meteorological Society, https://doi.org/10.1002/qj.3803, 2020.

Hofer, S., Lang, C., Amory, C., Kittel, C., Delhasse, A., Tedstone, A., and Fettweis, X.: Greater Greenland Ice Sheet contribution to global sea level rise in CMIP6, Nature communications, 11, 1–11, https://doi.org/10.1038/s41467-020-20011-8, 2020.

Howat, I., Negrete, A., and Smith, B.: MEaSUREs Greenland Ice Mapping Project (GIMP) Digital Elevation Model from GeoEye and WorldView Imagery, Version 1 [Data Set], https://doi.org/10.5067/H0KUYVF53Q8M, last access 09-15-2022, 2017.

Howat, I. M., Negrete, A., and Smith, B. E.: The Greenland Ice Mapping Project (GIMP) land classification and surface elevation data sets, The Cryosphere, 8, 1509–1518, https://doi.org/10.5194/tc-8-1509-2014, 2014.

Hutter, K.: Theoretical Glaciology, D, 1, Reidel Publishing Company/Terra Scientific Publishing Company, Reidel, Japan, 1983.

Johnson, J., Hand, B., and Bocek, T.: Greenland Standard Data Set, http://websrv.cs.umt.edu/isis/index.php/Present_Day_Greenland/Greenland_5km_v1.1.nc, last access 09-15-2022, 2019.

Joughin, I., Smith, B. E., and Howat, I. M.: A complete map of Greenland ice velocity derived from satellite data collected over 20 years, Journal of Glaciology, 64, 1–11, https://doi.org/10.1017/jog.2017.73, 2018.

Kittel, C., Amory, C., Agosta, C., Jourdain, N. C., Hofer, S., Delhasse, A., Doutreloup, S., Huot, P.-V., Lang, C., Fichefet, T., and Fettweis, X.: Diverging future surface mass balance between the Antarctic ice shelves and grounded ice sheet, The Cryosphere Discussions, pp. 1–29, https://doi.org/10.5194/tc-15-1215-2021, 2020.

Le clec'h, S., Charbit, S., Quiquet, A., Fettweis, X., Dumas, C., Kageyama, M., Wyard, C., and Ritz, C.: Assessment of the Greenland ice sheet–atmosphere feedbacks for the next century with a regional atmospheric model coupled to an ice sheet model, The Cryosphere, 13, https://doi.org/10.5194/tc-13-373-2019, 2019.

https://doi.org/10.5194/tc-2023-15
Preprint. Discussion started: 15 February 2023

Meehl, G. A., Senior, C. A., Eyring, V., Flato, G., Lamarque, J.-F., Stouffer, R. J., Taylor, K. E., and Schlund, M.: Context for interpreting equilibrium climate sensitivity and transient climate response from the CMIP6 Earth system models, Science Advances, 6, 1–10, https://doi.org/10.1126/sciadv.aba198, 2020.

Morland, L. W., Der Veen, C. J. V., and Oerlemans, J.: Dynamics of the West Antarctic ice sheet, Cambridge University Press, Cambridge, UK and New York, NY, USA, 1987.

O'Neill, B. C., Tebaldi, C., van Vuuren, D., Eyring, V., Friedlingstein, P., Hurtt, G., Knutti, R., Kriegler, E., Lamarque, J.-F., Lowe, J., Meehl, G. A., Moss, R., Riahi, K., and Sanderson, B. M.: The Scenario Model Intercomparison Project (ScenarioMIP) for CMIP6, Geoscientific Model Development, 9, 3461–3482, https://doi.org/10.5194/gmd-9-3461-2016, 2016.

Oppenheimer, M., Glavovic, B., Hinkel, J., van de Wal, R., Magnan, A., Abd-Elgawad, A., Cai, R., Cifuentes-Jara, M., DeConto, R., Ghosh, T., Hay, J., Isla, F., Marzeion, B., Meyssignac, B., and Z., S.: Sea Level Rise and Implications for Low-Lying Islands, Coasts and Communities, in: IPCC Special Report on the Ocean and Cryosphere in a Changing Climate, edited by Pörtner, H.-O., Roberts, D., Masson-Delmotte, V., Zhai, P., Tignor, M., Poloczanska, E., Mintenbeck, K., Alegría, A., Nicolai, M., Okem, A., Petzold, J., Rama, B., and Weyer, N., 2019.

Riahi, K., van Vuuren, D. P., Kriegler, E., Edmonds, J., O'Neill, B. C., Fujimori, S., Bauer, N., Calvin, K., Dellink, R., Fricko, O., Lutz, W., Popp, A., Cuaresma, J. C., KC, S., Leimbach, M., Jiang, L., Kram, T., Rao, S., Emmerling, J., Ebi, K., Hasegawa, T., Havlik, P., Humpenöder, F., Da Silva, L. A., Smith, S., Stehfest, E., Bosetti, V., Eom, J., Gernaat, D., Masui, T., Rogelj, J., Strefler, J., Drouet, L., Krey, V., Luderer, G., Harmsen, M., Takahashi, K., Baumstark, L., Doelman, J. C., Kainuma, M., Klimont, Z., Marangoni, G., Lotze-Campen, H., Obersteiner, M., Tabeau, A., and Tavoni, M.: The Shared Socioeconomic Pathways and their energy, land use, and greenhouse gas emissions implications: An overview, Global Environmental Change, 42, 153–168, https://doi.org/10.1016/j.gloenvcha.2016.05.009, 2017.

Robinson, A., Calov, R., and Ganopolski, A.: Greenland ice sheet model parameters constrained using simulations of the Eemian Interglacial, Climate of the Past, 7, 381–396, https://doi.org/10.5194/cp-7-381-2011, 2011.

Van den Broeke, M. R. and Gallée, H.: Observation and simulation of barrier winds at the western margin of the Greenland ice sheet, Quarterly Journal of the Royal Meteorological Society, 122, 1365–1383, https://doi.org/10.1256/smsqj.53406, 1996.

Vandecrux, B., Mottram, R., Langen, P. L., Fausto, R. S., Olesen, M., Stevens, C. M., Verjans, V., Leeson, A., Ligtenberg, S., Kuipers Munneke, P., Marchenko, S., van Pelt, W., Meyer, C. R., Simonsen, S. B., Heilig, A., Samimi, S., Marshall, S., Machguth, H., MacFerrin, M., Niwano, M., Miller, O., Voss, C. I., and Box, J. E.: The firn meltwater Retention Model Intercomparison Project (RetMIP): evaluation of nine firn models at four weather station sites on the Greenland ice sheet, The Cryosphere, 14, 3785–3810, https://doi.org/10.5194/tc-14-3785-2020, 2020.

Vizcaíno, M., Mikolajewicz, U., Jungclaus, J., and Schurgers, G.: Climate modification by future ice sheet changes and consequences for ice sheet mass balance, Climate Dynamics, 34, 301–324, https://doi.org/10.1007/s00382-009-0591-y, 2010.

Winkelmann, R., Martin, M. A., Haseloff, M., Albrecht, T., Bueler, E., Khroulev, C., and Levermann, A.: The Potsdam Parallel Ice Sheet Model (PISM-PIK) – Part 1: Model description, The Cryosphere, 5, 715–726, https://doi.org/10.5194/tc-5-715-2011, 2011.